Multiviews Reconstruction for Prosthetic Design

Nasrul Mahmood[1], Camallil Omar[2], and Tardi Tjahjadi[3]
[1,2]Faculty of Electrical Engineering, Universiti Teknologi Malaysia, Malaysia
[3]School of Engineering, University of Warwick, United Kingdom

Abstract: *Existing methods that use a fringe projection technique for prosthetic designs produce good results for the trunk and lower limbs; however, the devices used for this purpose are expensive. This paper investigates the use of an inexpensive passive method involving 3D surface reconstruction from video images taken at multiple views. The method that focuses on fitting the reference model of an object to the target data is presented. For an upper dummy limb, the fitting of the model with the data shows a satisfactory result. The results of 15 measurements of different length between both reconstructed and actual dummy limb are highly correlate. The methodology developed is shown to be useful for prosthetic designers as an alternative to manual impression during the design.*

Keywords: *3D Surface reconstruction, orthotic prosthetic.*

Received April 7, 2009; accepted March 9, 2010

1. Introduction

Three-Dimensional (3D) digitalisation systems applied to the orthopaedic domain allow for the freeing from the necessity of making manual impressions of the socket during orthotic and prosthetic design. The work carried out in these fields aims to find the best fitting of the socket into the portion of the arm or leg remaining after an amputation (residual limb or stump), during the prosthetic design. A prosthetic device (also called a prosthesis) is an artificial substitute for a missing body part such as an arm, leg, hand or foot, and is used for functional or cosmetic reasons, or both [6, 8].

Most of the previous works on prosthetic design are based on manual design and use Computer-Aided Design/Computer-Aided Manufacturing (CAD/CAM) systems. With a manual design, the most common way of defining the shape of a residual limb is to make a mould of the residual limb itself. A trained practitioner can then manipulate the mould in order to correctly spread out the pressure that the mould exerts on the patient. A milling or carving machine is used to transform the physical model into a foam or plaster shape, which is finally used on the patient as a medical support device [6]. This method is prone to deviations caused by human error. One of the advantages in computer-aided design is the reduced need for cast modifications and is, thus, a time saver. However, computer-aided systems increase the initial cost and training that is needed to operate the system. This initial cost and training is decreased if there is a system that can capture the residual limb shapes and give the actual dimension of the limb for the design. This can be realised using a reconstructed image [10, 11] of the limb for orthotic and prosthetic design. The cost of training will be reduced as the image is analysed automatically. Using the reconstructed 3D image would also be more comfortable for the patient when compared to using a traditional fabrication, as the latter might cause more injury during the design.

The scope of this paper is to provide a system which uses a 3D reconstruction technique that is capable of producing the measurement of the limb and creating a model of the limb in order to provide a prosthetist with an easy and yet accurate means of measuring a residual limb and creating a model of the missing part of the limb.

2. Surface Reconstruction from Multiviews

In this paper, the perspective camera model is used. This corresponds to an ideal pinhole camera [2, 4]. The process is completely determined by choosing a perspective projection/camera centre C and an image plane R. The projection of a scene point M is then obtained as the intersection of a line connecting this point and the centre of the projection C with the image plane, as shown in Figure 1. The optical axis is the line going through C perpendicular to the image plane R. It pierces that plane at the principal point p. An orthonormal system of coordinates in an image plane centred at p is used to define a 3D orthonormal system of coordinates (called the camera coordinate system) and is centred at the projection centre C with two axes of coordinates parallel to the image plane and the third parallel to the optical axis. The focal length f is the distance between point C and image plane R.

The relationship between the coordinates of M, $[X, Y, Z]^T$ and those of its projection m, i.e., $[x, y]^T$, is given by the Tales theorem [2]:

$$x = f \bullet \frac{X}{Z} \qquad y = f \bullet \frac{Y}{Z} \tag{1}$$

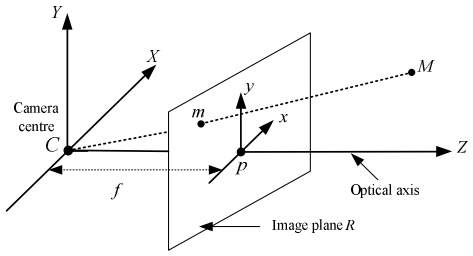

Figure 1. The pinhole camera model.

A point *m* in an image represents an incoming light ray; called the optical ray of *m*. By definition, the optical ray contains the optical centre. Therefore, to define its position in 3D in the camera coordinate system, we just need to specify another point along the ray, say coordinates $[X, Y, Z]^T$. However, any point of coordinates $[\lambda X, \lambda Y, \lambda Z]^T$ represents the same ray, since it is projected to the same 2D point *m*. The projective coordinates of *m* are $[x, y, 1]^T$, so we see that these projective coordinates represent a point in 3D on the optical ray of *m*. This property remains true if another triplet of equivalent projective coordinates is used. Using the homogeneous representation of a point, a linear projection equation is obtained:

$$m = \begin{bmatrix} x \\ y \\ 1 \end{bmatrix} = \begin{bmatrix} 1 & 0 & 0 & 0 \\ 0 & 1 & 0 & 0 \\ 0 & 0 & 1 & 0 \end{bmatrix} \begin{bmatrix} X \\ Y \\ Z \\ 1 \end{bmatrix} \quad (2)$$

Where (X,Y,Z) is a world point and (x,y) is the corresponding image point.

2.1. Shape from Silhouette

The earliest attempts in reconstructing 3D models from photos used the silhouettes of objects as sources of shape information [5]. A 2D silhouette is the set of closed contours that outline the projection of the object onto the image plane. By the principle of perspective projection, an object has to lie within the cone (bounding volume) formed by its silhouette from the corresponding camera viewpoint, as shown in Figure 2. Typically, shape from silhouette techniques start with an acquisition step where images of the object are taken from different locations around it. For each of these images, the object silhouette is extracted using simple differencing or image segmentation techniques.

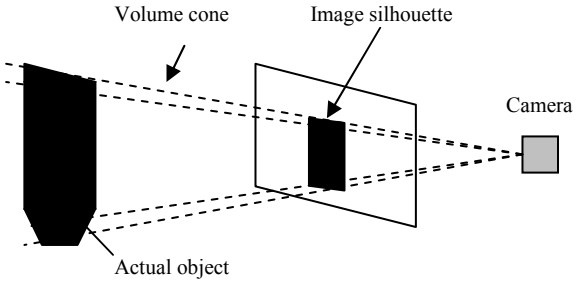

Figure 2. Bounding volume constraints of shape from silhouette.

The computed silhouettes for every image along with the centre of the corresponding camera are then used to define a volume, which if back-projected to 3D space can be assumed to bound the object. The intersection of these volumes associated with the set of acquired images yields a reasonable approximation of the real object. This intersection volume was named the 'visual hull' by [3] and described as the maximal object that gives the same silhouette with the real object from any possible viewpoint.

Silhouettes of an object in motion are employed in order to improve accuracy in the reconstructed shape. In some related works, the object is observed by cameras while being rotated by turntables [3, 9]. Obtained images of the object in rotation can be applied to the volume intersection method. Changing relative positions between the cameras and the object is described by the rotation parameter of a turntable.

2.2. Approximate Circular Motion

In circular motion, the camera's internal parameters remain identical over the whole image sequence [9]. This facilitates the camera calibration process by enabling the camera's parameters to be estimated using the same internal parameters and 3D camera position with respect to the reference camera position. In turntable motion, the physical imperfection of the turntable as well as measurement error affected the accuracy of object reconstruction. Hence, a modified projection matrix is used. If circular motion is assumed, then a projection matrix at a rotated position α, P (α), is:

$$P(\alpha) = KR[R(\alpha) \quad -\vec{o}_\alpha] \quad (3)$$

Where *K* is a 2D affine homography which includes the internal parameters of a camera and *R* is the 3D rotation matrix relating the world frame and camera frame. The 2D similarity homography *R(α)* represents a pure 2D rotation term of the circular motion. The 3D camera origin with respect to the world frame is represented as $\vec{o}_\alpha$.

In Figure 3, $I(0)$ is a reference image plane, $I(\alpha)$ and $I(\alpha')$ respectively represent the estimated and true image plane which have been rotated by α degrees from o_{ref}. Although the true camera origin $o_{\alpha'}$ cannot be determined from images, the 2D homography between $I(\alpha)$ and $I(\alpha')$ is estimated when there are at least four pairs of correspondence, i.e., $x^{\alpha'} \leftrightarrow x^w$, where:

$$x^{\alpha'} = H_p KR[R(\alpha) \quad -\vec{o}_\alpha] x^w \quad (4)$$

and H_p is designed as a projective homography having 8 degrees of freedom because the lines at infinity $\vec{l}_h$ in $I(\alpha)$ and $I(\alpha')$ are not identical.

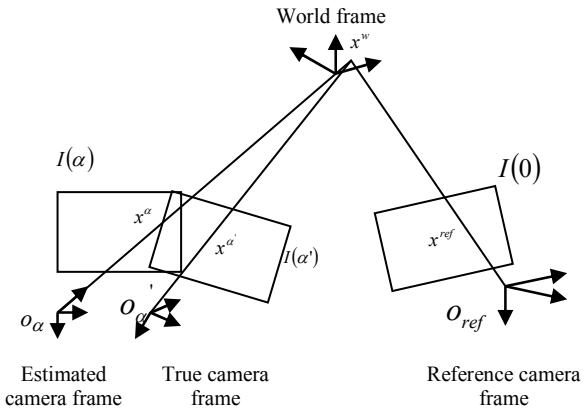

Figure 3. Geometrical illustration of circular motion.

Using the Direct Linear Transform algorithm when more than 4 points are detectable to derive a linear solution of H_p, the modified projection matrix for an approximate circular motion can be formulated as:

$$P'(\alpha) = H'_p[R(\alpha) \quad -\vec{o}_{\alpha}] \tag{5}$$

Where $H'_p = H_p KR$.

The following decision function of two projection matrices is:

$$d\left(P(\alpha), P'(\alpha)\right) = \sum_i \left\| \left(P(\alpha) - P'(\alpha)\right) x_i^w \right\| \tag{6}$$

Introduced in order to achieve an accurate object reconstruction. If $d\left(P(\alpha), P'(\alpha)\right)$ is greater than zero, then $P'(\alpha)$ replaces $P(\alpha)$ otherwise the estimated projection matrix remains unchanged.

3. Surface Deformation in Reconstruction Process

A model-based 3D reconstruction technique that can generate a patient-specific and detailed 3D surface model from multiviews images is introduced. Since the limb shape variances make it difficult to extract the feature and segment, a reference model provides important prior knowledge for reconstruction. The final model is obtained by deforming the reference model with constraints imposed by the shape from the silhouette result. There are two methods used for obtaining the reference model of the limb and others similar to the limb object. First, using the octree data from 3D reconstruction technique [9] and secondly, the data created by computer programming.

A digital camera is used in this paper because instead of the vast capability, it is widely used in computer graphics, a relatively small device and cheaper than contact methods or a laser scanner, easy to handle and has the freedom of movement to capture object images from multiviews. Since the involved data are two data sets (the reference model (model) and the target objects (data)), the data need to be registered in order to merge them into a complete set of points in single views before the deformation process can be done between both data sets. To achieve that, the Iterative Closest Point (ICP) algorithm is used [1, 7]. The point set of the data shape is rigidly moved (registered and positioned) to be in best alignment with the model shape. This is done iteratively. In the first step of each iteration, the closest point on the surface of the model is computed for every data point. This is the most time consuming part of the algorithm and has to be implemented efficiently. As a result of this first step, one obtains a point sequence $Y = (y_1, y_2, ...)$ of closest model shape points to the data point sequence $X = (x_1, x_2, ...)$. Each point x_i corresponds to the point y_i with the same index. In the second step of each iteration, the rigid motion *m* is computed such that the moved data points *m* (x_i) are closest to their corresponding points, y_i, where the objective function to be minimized is:

$$F = \sum_{i=1}^{N} \left\| m(x_i) - y_i \right\|^2 \tag{7}$$

This least squares problem can be solved explicitly. The translational part of *m* brings the centre mass of *X* to the centre mass of *Y*. The rotational part of *m* can be obtained as the unit eigenvector that corresponds to the maximum eigenvalue of a symmetric 4×4 matrix. The solution eigenvector is nothing but the unit quaternion description of the rotational part of *m*. After this second step, the positions of the data points are updated via $X_{new} = m(X_{old})$. Now, step 1 and step 2 are repeated, always using the updated data points, until the change in the mean-square error falls below a preset threshold. Since the value of the objective function decreases both in steps 1 and 2, the ICP algorithm always converges monotonically to a local minimum.

After registration, pre-processing takes place to establish the correspondence between both registered data sets to find the feature points on the reference model (model) that correspond to the points on the target objects (data). Although the registration between two datasets produces good results, correspondence establishment is needed because ICP only does the rigid registration and there is no non-rigid movement or re-sampling of the vertices. A reference model point is the corresponding point of the data shape if both points are projected to the same location on the intermediate object. In the proposed algorithm, the cylinder with the unit radius is used as the intermediate object.

After the correspondence between the reference model and data is established, the reference model is deformed to match the data. In the proposed algorithm, the object surface defines an influence

region rather than being within a 3D volume. The proposed algorithm solves the problem where two points are close by Euclidean distance, however remote by surface distance. The influence region of a constraint point consists of all the points on the reference model whose surface distances to the constraint point are smaller than a given radius. The surface distance between two points is calculated by adding all the distance along triangle on the shortest surface path between them. The deformation is calculated by accumulating the influences propagated through neighbouring points.

For the established correspondence, each data point is paired with a reference model feature point. Therefore, the displacement of a feature point can be calculated by:

$$d(C) = \|K - C\| \tag{8}$$

Where $d(C)$ is the displacement vector of feature point C, and K is the corresponding data point of C.

A point only has direct influence on its neighbouring points. Let C be a feature point and P be one of C's neighbouring points. Hence, the displacement of P is given by:

$$d(P) = d(C) * f\left(\frac{\|P - C\|}{r}\right) \tag{9}$$

Where $f(x)$ is a decreasing function with $f(0) = 1$ and $f(x) = 0$ for $x \geq 1$; r is the radius of an influence region. $f(x)$ is equal to zero for $\|P - C\| \geq r$ (points whose distance from C is greater than or equal to the radius r) and $f(x)$ is equal to 1 when $\|P - C\| = 0$ (the feature point itself). Point P will in turn influence its own neighbouring points, using (9) again. But this time, P takes the place of feature point C in the equation. This process continues until the displacement of P, $d(P)$ drops below a given threshold t or the surface distance between point P and feature point C exceeds C's influence radius, R_c.

Let P_n be any point that is influenced by feature point C, and $P_1, P_2, ..., P_{n-1}$ the points on the surface path between P_n and C. The displacement of P_n is thus obtained by:

$$d(P_n) = d(C) * f\left(\frac{\|P_1 - C\|}{r}\right) * f\left(\frac{\|P_2 - P_1\|}{r}\right) * \ldots f\left(\frac{P_n - P_{n-1}}{r}\right) \tag{10}$$

Where * is a convolution.

4. Results and Discussion

The results are obtained by using Visual C++ (Ver. 6.0) with some OpenGL environment. The proposed method for the deformation process was applied to six different objects, which included the dummy lower and upper limbs. Table 1 summarised the percentage of non-matching vertices for these six objects after the deformation process. The table shows that for a large number of object vertices (candle) and the object which have lot of sharp corner (fruit), it is difficult to fit their model to the data. Both of these objects almost have a half percentage of non-matching vertices after the deformation process which are 50% for a candle and 47% for a fruit. The rest of the objects have below 30% of non-matching vertices and are considered low. However, there are plenty of opportunities to improve this percentage.

The experimented results show that the movement of model vertices to fit the data vertices depends on some of the cases below:

1. If a few vertices' locations are different, the method performs very well, where almost all the vertices can fit or move towards the data.
2. As the differences between the model and the data vertices increase, it becomes difficult for the model to fit to the data.
3. For a dummy limb, the fitting of the model with the data shows a satisfactory result. The results of 15 measurements show that both the upper and lower limbs have a correlation coefficient close to 1, i.e., both the model and the actual limb data are highly correlated.

Table 1. The percentage of non-matching vertices of six objects.

Objects	Non-Matching Vertices (Approx.)	Total Registered Vertices (Approx.)	Percentage of Non-Matching Vertices (%)
Candle	47650	82156	58
Spherical Candle	1363	4808	28
Box	900	4200	21
Fruit	3094	6584	47
Lower Limb	1720	6373	26
Upper Limb	1023	4265	24

In prosthetic design, it is necessary to perform quantitative analysis and measurements. The length, angle, area of region, 3D surface area and volume of the limb are measured. The analysis and measurements are employed to ensure that the 3D model created will fit the actual data. It is helpful for the designer to design an appropriate size of the model prosthetic limb, where it is subsequently modified during the design. For the upper limb, the results shows that 24% of vertices are not match correctly after the deformation process. There are about 1023 vertices did not registered properly compare to 4265 vertices are well registered. As a result, there are plenty of opportunities to improve this percentage.

In order to evaluate the result, the modified 3D model which has been created after the deformation process and the actual limb data are compared. The evaluation is done by comparing some selected points of the actual object with the size of the object created by the deformation process (the modified 3D data). In

order to present the modified 3D model after the deformation process, *Matlab 7* is used. After the grid is manually drawn, as shown in Figure 4, the actual limb is positioned to correspond to the modified 3D data in Figure 5.

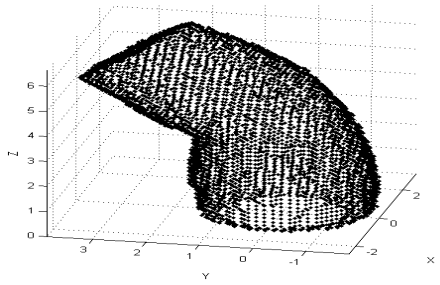

Figure 4. Modified 3D model of an upper dummy limb after deformation process.

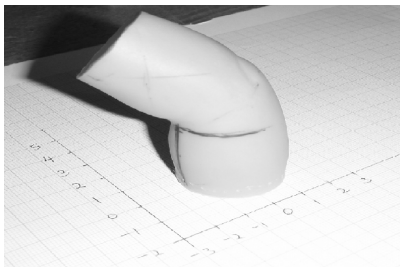

Figure 5. Measuring the approximate position of an actual dummy limb.

Next, the procedure of measuring the cross-sections and comparing those of the modified 3D model and actual limb is performed. The first corresponding feature point used is the sharp corner of the limb. In Figure 6, the modified 3D model is displayed with the z and y axes as starting points to calculate the length measurement for comparison with the actual limb. This is because the 3D point (0.7813, 1.563, 2.734), as shown in Figure 6, is the most obvious point that can be determined in both the 3D model and actual limb. The other lengths are measured and recorded in Table 2.

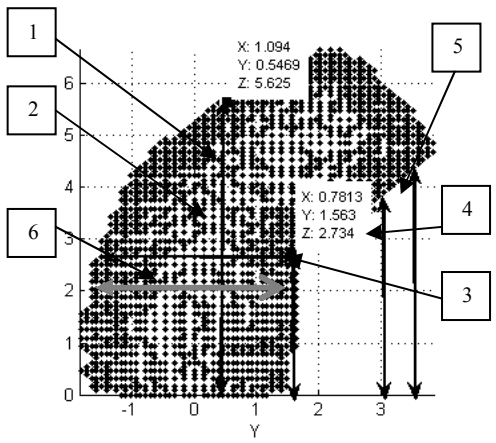

Figure 6. Z and y axis display of the modified 3D model. The labelled lines mark the measurement of the length in Table 2.

The modified 3D model display for different views is shown in Figure 7 for the z and x axes and in Figure 8 for the x and y axes.

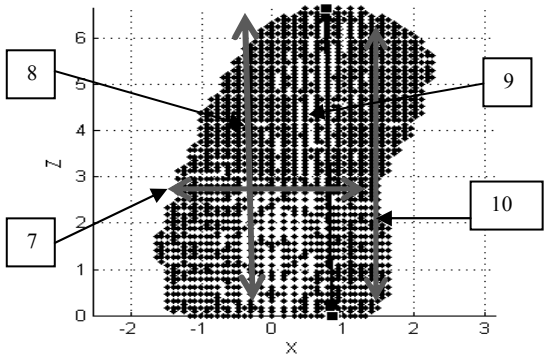

Figure 7. Z and x axis display of the modified 3D model. The labelled lines mark the measurement of the length in Table 2.

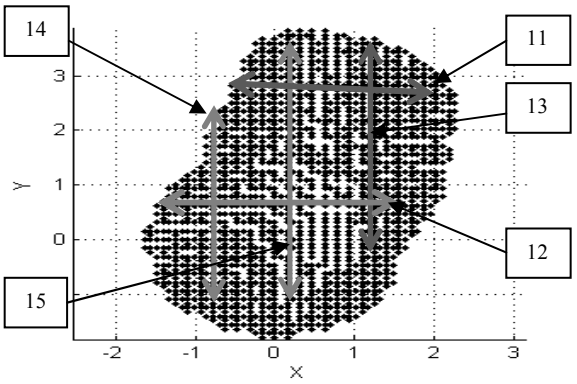

Figure 8. X and y axis display of the modified 3D model. The labelled lines mark the measurement of the length in Table 2.

The fifteen measurements and comparisons between the modified 3D data and actual limb are shown in Table 2.

Table 2. Differences between the modified model and the upper limb data.

Length	Modified 3D Model (cm)	Actual limb (cm) ± Errors	Difference (cm) ± Errors
1	5.6	5.5 ± 0.2	0.1 ± 0.2
2	3.0	2.8 ± 0.1	0.2 ± 0.1
3	2.9	2.9 ± 0.2	0.0 ± 0.2
4	3.8	3.8 ± 0.1	0.0 ± 0.1
5	4.6	4.5 ± 0.3	0.1 ± 0.3
6	3.9	3.9 ± 0.2	0.0 ± 0.2
7	3.2	3.2 ± 0.1	0.0 ± 0.1
8	6.1	6.0 ± 0.1	0.1 ± 0.1
9	6.8	6.8 ± 0.1	0.0 ± 0.1
10	3.1	3.0 ± 0.2	0.1 ± 0.2
11	2.8	2.9 ± 0.1	0.1 ± 0.1
12	3.6	3.6 ± 0.1	0.0 ± 0.1
13	3.8	3.8 ± 0.2	0.0 ± 0.2
14	2.5	2.4 ± 0.0	0.1 ± 0.0
15	3.9	3.7 ± 0.2	0.2 ± 0.2

From Table 2, the differences in length for several cross-sections of the modified 3D model and actual upper limb show a small difference, which means that the objective of fitting the model to the data during the deformation process has been adequately achieved. The correlation coefficient between 15 measurements of the modified 3D model and the actual limb is 0.99928. This shows that if prosthetic designers have chosen an appropriate design in order to fit the patient's residual limb, the proposed deformation process method could be used.

5. Conclusions

The results show how the method successfully handles the deformation process for an upper limb. Although the results show that 24% of vertices are not properly registered after deformation, the correlation coefficient between 15 measurements of the modified 3D model and actual limb proved that both modified 3D data is highly correlated with the actual limb. For real applications on the upper limb data, if the residual limb of a patient is already obtained the designers can use their database of previous data of residual limbs and fit these with the current patient's limb data. If the starting model is already similar to the limb data, then the deformation process achieves better performance. This offers advantages to the designer to find a good fit to design the orthotic and prosthetic limb. Future research could consist of improving the approach and developing it further. One of the important considerations is to apply the technique on real human limbs instead of using the dummy limbs of this paper. The reconstruction from multiviews in this paper uses a turntable system, which in practice is difficult for obtaining 3D data of real human limbs. In this case, rotating the camera instead of the object is a possible approach.

Acknowledgement

The authors would like to express their greatest gratitude to the Universiti Teknologi Malaysia and the Ministry of Higher Education of Malaysia for supporting this study.

References

[1] Besl P. and McKay N., "A Method for Registration of 3d Shapes," *IEEE Transactions on Pattern Analysis and Machine Intelligence*, vol. 14, no. 2, pp. 239-25, 1992.

[2] Faugeras O., *Three-Dimensional Computer Vision: A Geometric Viewpoint*, Massachusetts Institute of Technology Press, 1993.

[3] Fremont V. and Chellali R., "Turntable-Based 3D Object Reconstruction," *in Proceedings of IEEE Conference on Cybernetics and Intelligent Systems*, France, pp. 1277-1282, 2004.

[4] Hartley R. and Zisserman A., *Multiple View Geometry in Computer Vision*, Cambridge University Press, 1998.

[5] Laurentini A., "The Visual Hull Concept for Silhouettes-Based Image Understanding," *IEEE Transactions on Pattern Analysis and Machine Intelligence*, vol. 16, no. 2, pp. 150-162, 1994.

[6] Lusardi M. and Nielson C., *Orthotics and Prosthetics in Rehabilitation*, Elsevier, 2007.

[7] Rusinkiewicz S. and Levoy M., "Efficient Variants of the ICP Algorithm," *in Proceedings of 3rd Intelligence Conference on 3D Digital Imaging and Modeling*, CA, pp. 145-152, 2003.

[8] Seymour R., *Prosthetics and Orthotics-Lower Limb and Spinal*, Lippincott, Williams and Wilkins, 2002.

[9] Shin D. and Tjahjadi T., "3D Object Reconstruction From Multiple Views in Approximate Circular Motion," *in Proceedings of IEE SMK UK-RI Chapter Conference on Applied Cybernetics*, Selangor, pp. 70-75, 2005.

[10] Vincent C., Fournel T., and Fouquet R., "Self-Indexing of Multi-View Fringe Systems," *Computer of Journal Applied Optics*, vol. 42, no. 11, pp. 1981-1986, 2003.

[11] Wong K. and Cipolla W., "Structure and Motion from Silhouettes," *Technical Document Computer Vision*, pp. 217-222, 2001.

Nasrul Mahmood received his BSc and MSc degrees in electrical and electronic engineering from Universiti Kebangsaan Malaysia (UKM) and Universiti Teknologi Malaysia (UTM), respectively. He obtained his PhD degree in electrical engineering from the University of Warwick, UK. His research areas are 3D object reconstruction from video sequences and from multiple views, biomedical image processing and engineering rehabilitation. Currently, he is serving as a lecturer at the Faculty of Electrical Engineering, UTM.

Camallil Omar received his MSc in electrical engineering from University of Nottingham, UK. His research areas are electronic circuits and design, image processing, electronic instrumentation and medical electronics. He is now serving as a lecturer at the Faculty of Electrical Engineering, UTM for the past 20 years.

Tardi Tjahjadi received his BSc degree from University College London, and his MSc and PhD degrees from University of Manchester Institute of Science and Technology (UMIST). He has expertise in the areas of multiresolution image processing, object tracking and motion estimation, and 3D object reconstruction. He has published numerous papers in these areas. Currently, he is serving as an associate professor in the School of Engineering, University of Warwick, UK. He has been a senior member of IEEE since 2002.